Master's Thesis of Engineering

Effect of CO_2 Laser on Silicon Carbide (SiC) Polishing

실리콘 카바이드에 대한 CO_2 레이저 연마의 효과

August 2019

Graduate School of Seoul National University
College of Engineering
Department of Mechanical & Aerospace Engineering

Pablo Antonio Abrego Serrano

Effect of CO_2 Laser on Silicon Carbide (SiC) Polishing

Academic advisor Prof. Sung-Hoon Ahn

Submitting a master's thesis of Engineering

April 2019

Graduate School of Seoul National University
College of Engineering

Pablo Antonio Abrego Serrano

Confirming the master's thesis written by
Pablo Antonio Abrego Serrano
June 2019

Chair	Kunwoo Lee	(Seal)
Vice Chair	Sung-Hoon, Ahn	(Seal)
Examiner	Suk Won Cha	(Seal)

Abstract

Effect of CO_2 Laser on Silicon Carbide (SiC) Polishing

Pablo Antonio Abrego Serrano

Department of Mechanical and Aerospace Engineering

The Graduate School

Seoul National University

Silicon carbide (SiC) has long been recognized as an excellent material for high performance optical applications because it offers many advantages over other commonly used glasses and metals. Some of the superior attributes of SiC include extremely high specific stiffness (E/ρ), high thermal conductivity and outstanding dimensional stability.

The effect of and CO_2 laser and its tool path on silicon carbide (SiC) were investigated. The process started by creating Laser induced cracks on the desired pattern. Subsequently, laser assisted polishing was conducted on the same tool path. The surface showed a sharp difference in material removal in the areas with laser induced cracks and in areas with no cracks. This high difference in material removal was used to generate macro and micro patterns. Grooves from 2 mm to 200 μm in width and 5 μm to 20 μm depth were successfully generated. Moreover, this process was used to machine a spherical concave mirror that was later used as part of a Newtonian telescope.

Keyword : Polishing, Hybrid, Material Removal Rate (MRR), Patterning

Student Number : 2017-26782

Table of Contents

List of Tables

List of Figures

Chapter 1. Introduction

1.1. Purpose of Research

Some of the preferred characteristics for an optical mirror material include low density, high elastic modulus, low coefficient of thermal expansion, and high thermal conductivity [1-5]. Depending upon the specific use, the fracture toughness and stress corrosion constant, which control slow crack growth and long-term reliability under static or dynamic loads during manufacturing and use, may also be important.

Silicon carbide (SiC) has long been recognized as an excellent material for high performance optical applications because it offers many advantages over other commonly used glasses and metals [6-8]. Some of the superior attributes of SiC include extremely high specific stiffness (E/ρ), high thermal conductivity and outstanding dimensional stability as shown in Table 1 [1].

Table 1. Mechanical Properties of Silicon Carbide (SiC)

Parameter [unit]	Value
Density (gm/cc)	3.1
Porosity (%)	0
Flexural Strength (MPa)	550
Elastic Modulus (GPa)	410
Compressive Strength (MPa)	3900
Hardness (Kg/mm2)	2800
Fracture Toughness (MPa•m1/2)	4.6
Maximum Use Temperature (°C)	1650
Thermal Conductivity (W/m•°K)	120
Coefficient of Thermal Expansion (10-6/°C)	4
Specific Heat (J/Kg•°K)	750
Hardness (Kg/mm2)	2800

.

Because silicon carbide is an extremely hard and strong material, the precision machining required for both shaping and light

weighting is typically performed with diamond tooling on very stiff high quality machine tools (e.g., precision CNC equipment) using slow (comparatively speaking) material removal profiles. Conventional finishing processes (lapping, polishing) of SiC substrates also proceed much more slowly when compared to conventional optical materials due to the hardness and fracture toughness of the material. Even with the necessary use of diamond abrasive, the material removal rate for SiC is approximately 1/35th that of fused silica and less than 1/50th that of Zerodur[①]. Compounding these issues, any light weighting of the substrate can induce additional difficulties for achieving high quality optical surface profiles (< λ/10).

Figure 1. Silicon Carbide Mirrors

Achieving such a high level of surface profile accuracy is often problematic, as the skilled optician requires multiple iterations of the polishing process to overcome such difficulties as print-through, accommodate unusual component geometries, etc. As a result, it is normally expensive to produce a light weighted, super-polished SiC

① lithium-aluminosilicate glass-ceramic produced by Schott AG since 1968. It has been used for a number of very large telescope mirrors including Keck I, Keck II, and SOFIA.

substrate, and the lead-time for obtaining a finished substrate can be several months. Thus, although SiC appears to be an ideal optical material from a material properties standpoint, the cost and lead-time associated with the preliminary shaping, light weighting, and optical finishing of the SiC substrate have heretofore been major impediments to the widespread use of the material in optical systems.

1.2. Surface Texture on Ceramics

Advanced ceramics are preferable for kinds of strategic application, low thermal conductivity, low coefficient of friction, excellent corrosion and wear resistance, high fracture toughness, and good thermal shock resistance make Silicon Carbide suitable for the use in engineering applications.

In order to improve tribological properties of ceramic surface, surface textures as an effective approach have been applied in bearings, mechanical seals and engine cylinder liners. Meanwhile, because of excellent tribological, electrical, and optical properties, ceramics with textures are also widely used in engineering applications such as cutting tools, solar receiver applications, and electronic component. However, the properties of ceramics have difficulties with respect to its engineering fabrication through traditional approaches.

Tires in automobiles are equipped with sophisticated surface textures to control friction for safe driving under various road conditions. Laser pre-treatment has been previously used to improve the tribological properties of ceramic surfaces [9-11],

1.3. Hybrid Machining Processes

Hybrid machining is combine different machining processes to manufacture components with a better machining performance. The objective of hybridizing processes is the positive effect of the hybrid process is more than double advantages of the single

processes [12–16]. Hybrid processes developing due to the advent of novel materials with extreme properties, requirements of enhanced machining precision and complex shaped parts which earlier difficult or not possible to machine with existing conventional and non–conventional machining technologies [17–20].

The term “hybrid process” in machining is related to the combination of different process energies or assisting a specific process by using another process energy. A hybrid process can be used in different terms:

1. Combination of different active energy sources which act at the same time in the processing zone (laserelectrochemical machining).

2. Processes which combine process steps that are usually performed in two or more process steps (grindhardening).

3. Hybrid machines, integrating different processes within one machining platform.

In this research, in order to increase the material removal rate (MRR) of Silicon Carbide (SiC) polishing, we combined polishing process with CO_2 laser machining. By combining this 2 processes, laser machining can increase the MRR and polishing process can guarantee a high surface quality (low surface roughness). Moreover, this process was used to fabricated surface patterns on SiC and to fabricate a concave spherical mirror for a Newtonian telescope.

Chapter 2. Experiment Set-up

2.1. Hardware set-up

As shown in Fig. 2, the experimental apparatus was installed to a simple 3-axis stage. The normal force was measured by dynamometer (Type 9251A, Kistler Inc., Germany) which was fixed on the bed. During the polishing process, the normal force was controlled by moving Z-axis upward/downward using feedback control. Slurry circulation system was also installed to supply sufficient abrasives.

As shown in Fig. 2, CO_2 laser beam system (LVI Technologies inc., Korea) was installed and laser was irradiated onto the material through two mirrors on the stage and one mirror inside the polishing tool for laser cracking and laser assisted polishing. The focus of the laser was adjusted to the material surface through a custom-made tool equipped with a mirror and a lens (50.8 mm Focal Length) inside. The duty cycle and pulse width of laser was controlled in order to generate pulsed laser and synchronize it through the rotating tool.

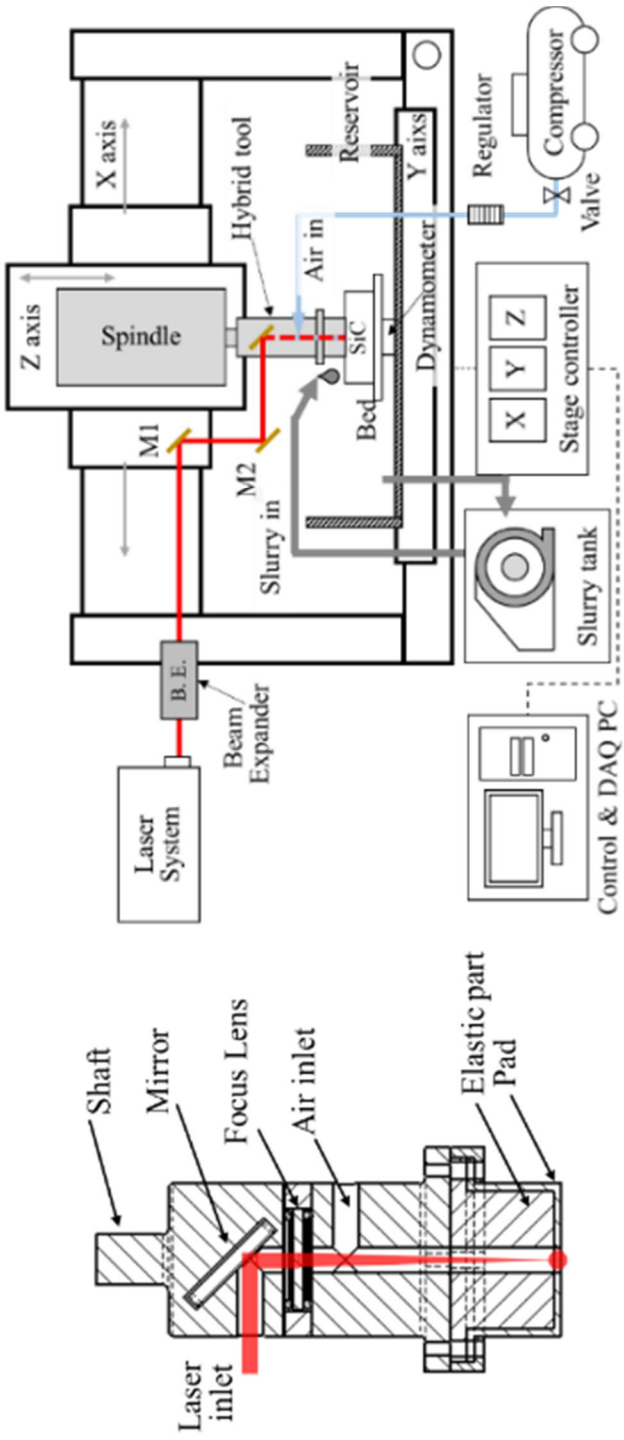

Figure 2 . Schematic diagram of the 'laser + polishing' hybrid process [21]

Chapter 3. Material Removal Rate

3.1. CO_2 laser generated cracks

The purchased silicon carbide was grinded by the manufacturer. The sample had grinding tool marks as shown in figure 3 (a). These grinding tool marks can be removed by simply polishing the sample for 40 to 60 minutes depending on the grinding tool mark's depth. After polishing by conventional method, the grinding tool marks were removed and surface roughness was reduced from R_a=1.356 mm to R_a=0.005 mm.

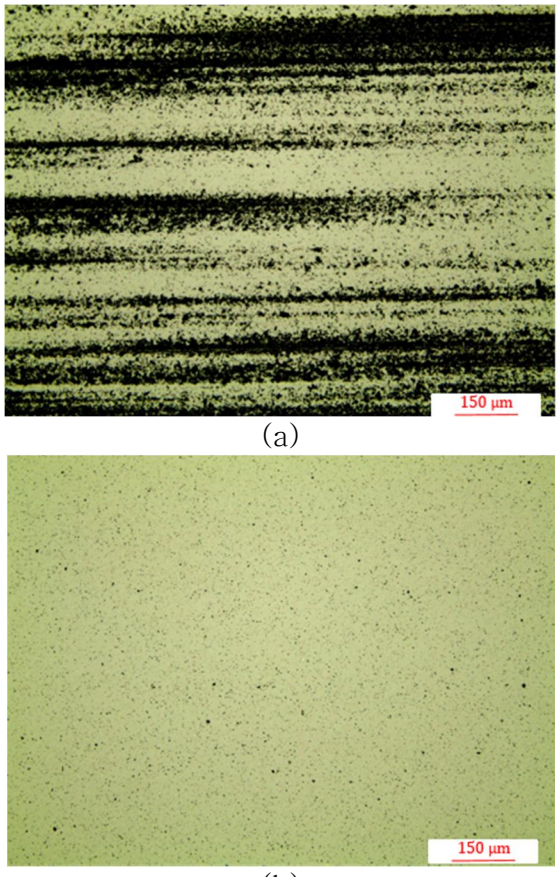

(a)

(b)

Figure 3. Microscope image of a SiC sample (a) polished for 10 minutes and (b) polished for 60 minutes.

By irradiating CO_2 laser on silicon carbide surface, cracks can be regenerated. Figure 4 (a) shows a SiC sample that was laser cracked and figure 4 (b) shows the surface of the same sample after 30 minutes of laser assisted polishing. As shown in the image, several black spots remained. These black marks are deep pits generated by the laser.

Figure 5 shows the differences between a surface that was polished without irradiating laser and a surface that was pre-cracked and subsequently laser assisted polished.

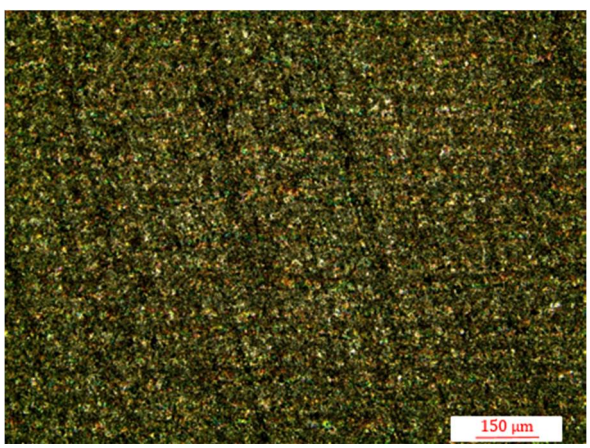

(a)

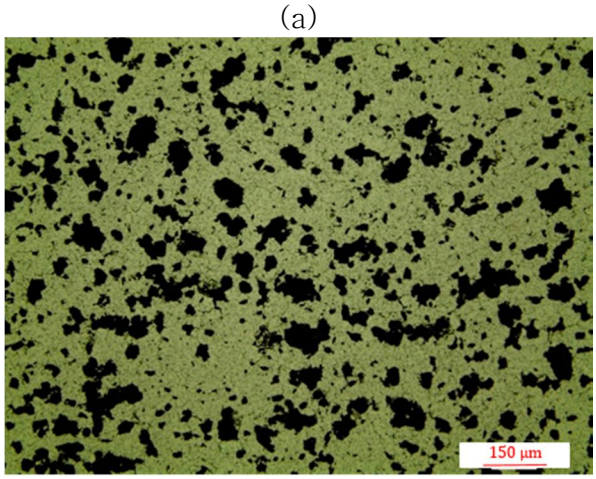

(b)

Figure 4. Microscope image of a SiC sample (a) laser cracked and (b) laser cracked + 60 minutes of polishing

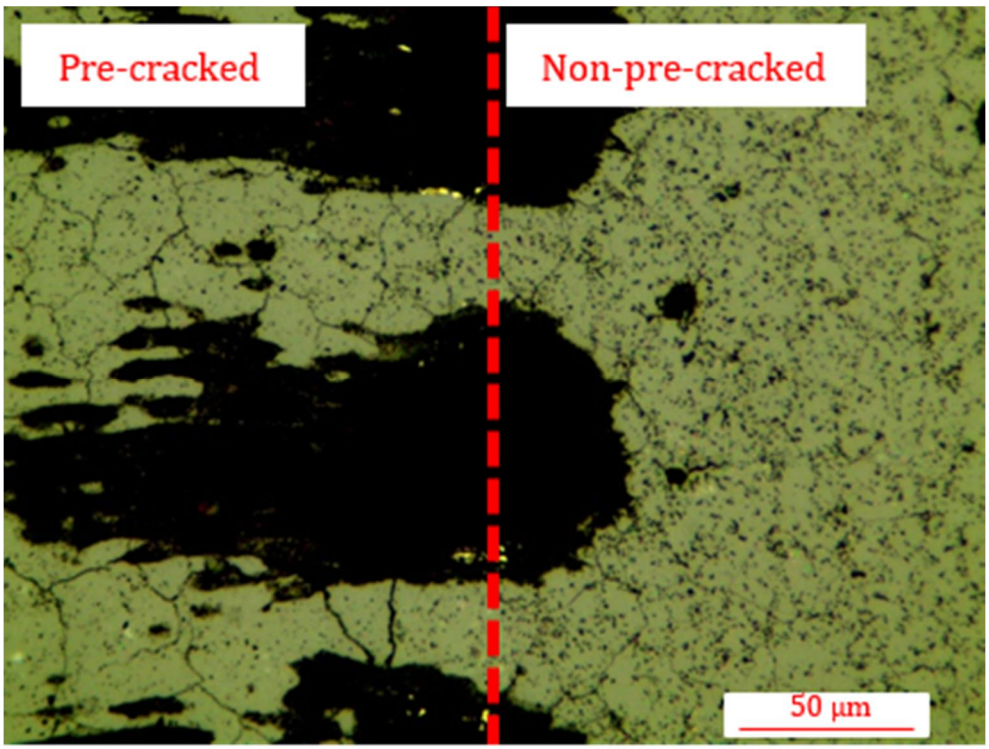

Figure 5. Microscope image showing difference between laser cracked surface and non-cracked

3.2. Experiment design

SiC samples with dimensions of 50 mm x 50 mm were used as the target for this experiment. A 0.05 mm width raster tool path with dimensions of 20 mm x 20 mm was used. Two different types of SiC samples were prepared: SiC as-received and laser pre-cracked sample. The tool size was 20 mm in diameter so the deepest polished point lays on the middle of the sample.

As shown in figure 6, an area of 40 mm x 40 mm was laser pre-cracked. Subsequently, a raster tool path of 0.05 mm width of 20 mm x 20 mm was used to perform the polishing process.

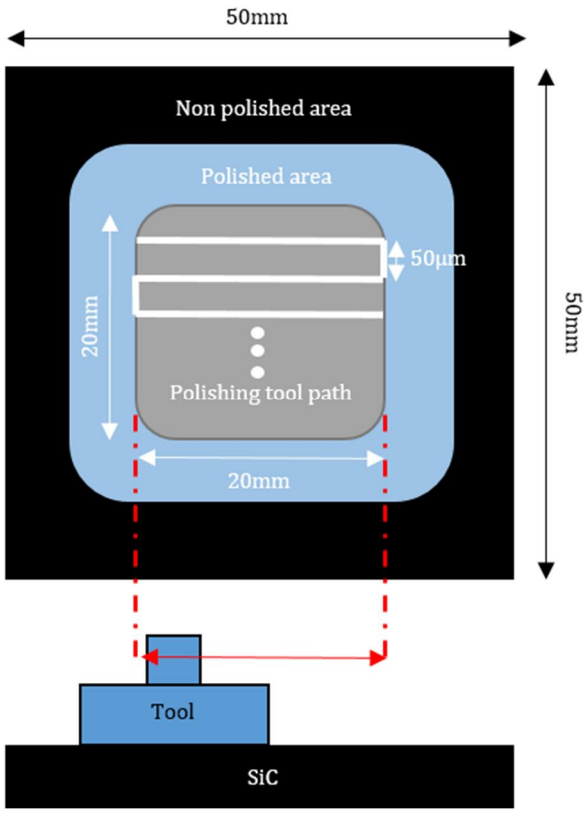

Figure 6. Diagram of MRR experiment's tool path

Four different types of experiments were performed, as shown in figure 7 to investigate the effect that each of them had on the material removal rate (MRR) of Silicon Carbide (SiC) polishing. Conventional polishing, laser assisted polishing (LAP), laser pre-cracks + laser assisted polishing (CLAP), and re-cracking which stands for the process in which laser pre-cracks are generated every 30 minutes.

The laser cracking process does not only create cracks on SiC surface but also evaporates some of the material. However, by using a 25% duty cycle which equals to 74.43 W, the evaporated material is negligible.

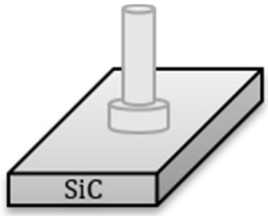

(a) Polishing

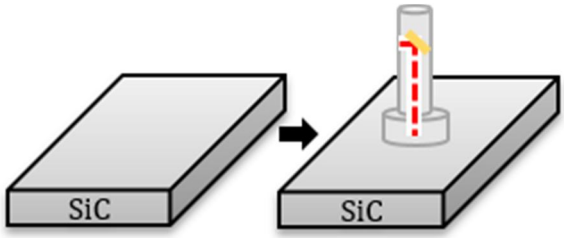

(b) LAP

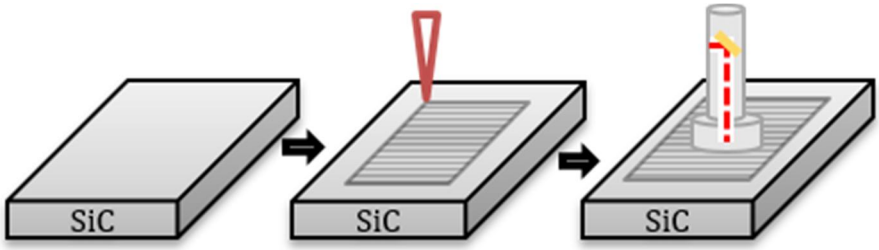

(c) CLAP

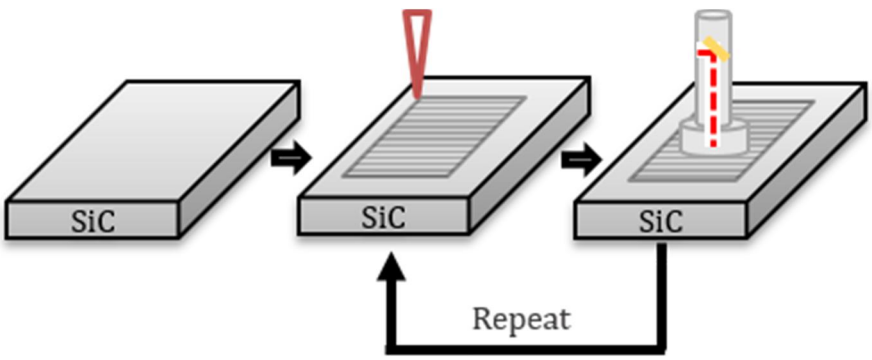

(d)Re-cracking + LAP

Figure 7. (a) conventional polishing (P), (b) laser assisted polishing (LAP), Pre-cracks + laser assisted polishing (CLAP), Re-cracking process [21].

Table 2. Experiment parameters

Work piece	Silicon carbide
Laser	
Source	CO_2 (wavelength 10.6 μm)
Type	Continuous wave
Power	77.43 W (Laser crack) 111.1 W (Laser assisted polishing)
Feed rate	25 mm/s
Polishing	
Tool diameter	20 mm
Force	18 N
Rotational speed	1,200 rpm
Slurry	Diamond and ceria (~1 μm)
Pad	Polyurethane
Feed rate	25 mm/s

3.3. Material Removal Measurement and Results

A surface profiler was used (Taylor Hobson, AMETEK inc.) to measure the maximum polished depth for each of the experiment's samples. Surface profiler can only measure the surface on a straight line, therefore it is not possible to know whether the surface was uniformly polished or not. In order to get an average value for the maximum polished depth, the surface was measured in 4 different directions as shown in figure 8.

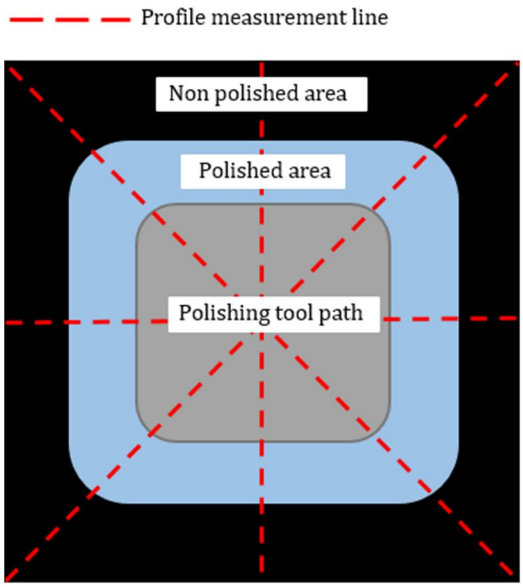

Figure 8. Diagram of the measurement of surface profile

Figure 9 shows the surface profiler data in 4 directions for CLAP process after 35 minutes of machining. As it can be seen, the profile is slightly different in some regions but overall it is very similar in all directions.

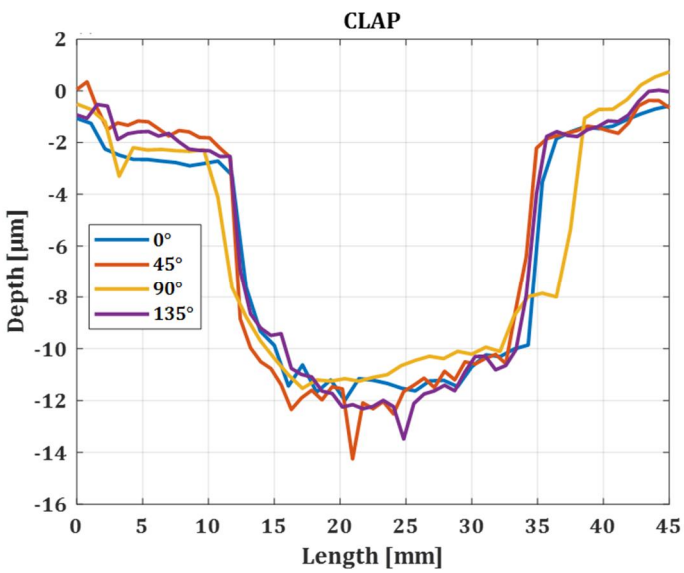

Figure 9. Surface profile data for CLAP process for the 4 different measured directions

Figure 10 shows that 19.4 um, 9.5 um and 8.9 um was the maximum polished depth for cracked + laser assisted polishing, laser (CLAP) assisted polishing (LAP) and conventional polishing (P) respectively. Conventional polishing and laser assisted polishing did not have much difference. However, laser cracks + laser assisted polishing showed a high MRR in the area where laser was irradiated during the polishing process.

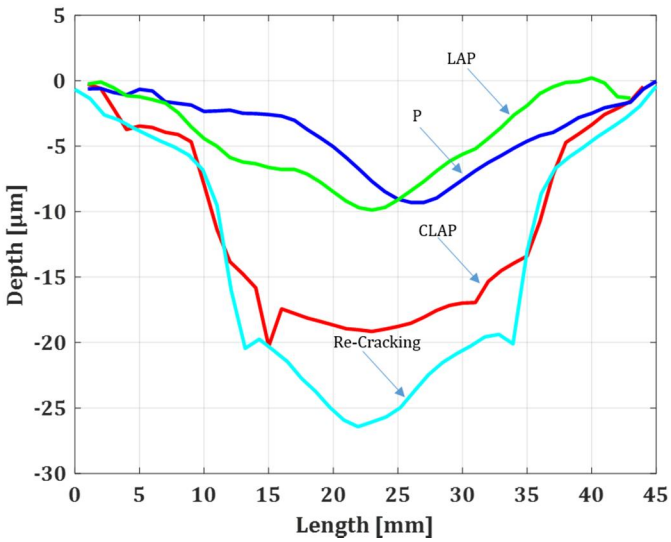

Figure 10. Surface profiler data for the 4 different performed experiments

The irradiated laser during laser assisted polishing seemed to have a higher effect on the pre-cracked surface. In order, to study the long term effect of pre-cracking and laser assisted polishing, re-cracking was done every 30 minutes. The process outline is described in figure 7 (d). First, the SiC as-received was cracked by laser, afterwards, the sample was laser assisted polished and after 30 minutes of polishing, the sample was cracked again by laser and subsequently polished again and this process was repeated. The maximum depth for this process was 26.5 um.

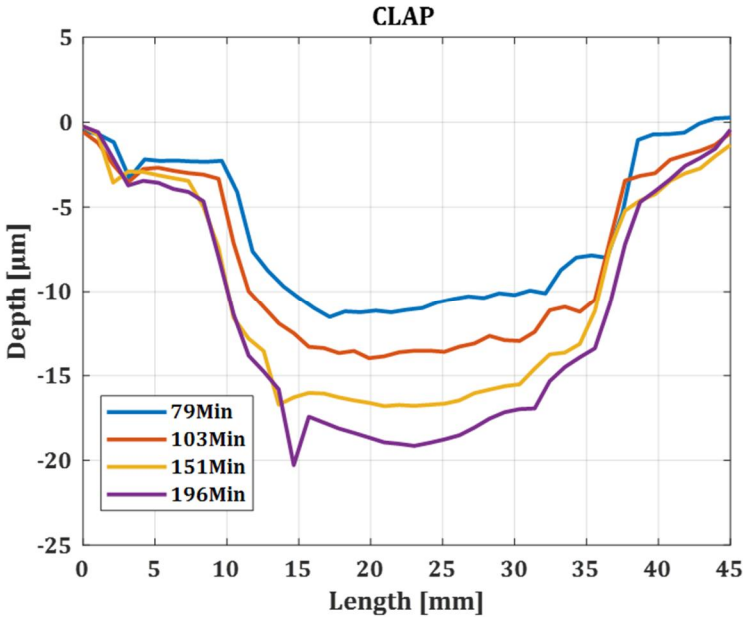

Figure 11. Surface profile data for re-cracking experiment over prolonged period of time

The results from the performed experiment in order to test the material removal rate over prolonged periods of time is shown in figure 11.

The maximum polished depth and material removal rate (MRR) for the 4 different experiments is shown in figure 12. For the conventional polishing process, we can see that the material removal stayed constant throughout the experiment. For the laser assisted polishing process, there is an increase of material removal at the early stage of the process but later on, the process's material removal rate becomes equal to the conventional process. In the case of the pre-cracked + laser assisted polishing process, there is a high increase of material removal rate on the early stage until a point when all initial cracks are removed. Finally, on the re-cracking process, the highest material removal rate occurs on the early stage but thanks to the re-cracking, more cracks are generated every time the sample is re-cracked and therefore increasing material removal rate. However, as seen in the CLAP and re-cracking process, the MRR decreases with time and becomes almost equal to the conventional polishing's MRR. The polishing

process has a characteristic of creating a high surface quality. This leads to create a surface with high reflectivity. Some of the laser that is irradiate on the surface is not absorbed and it is reflected. This explains why the MRR decreases.

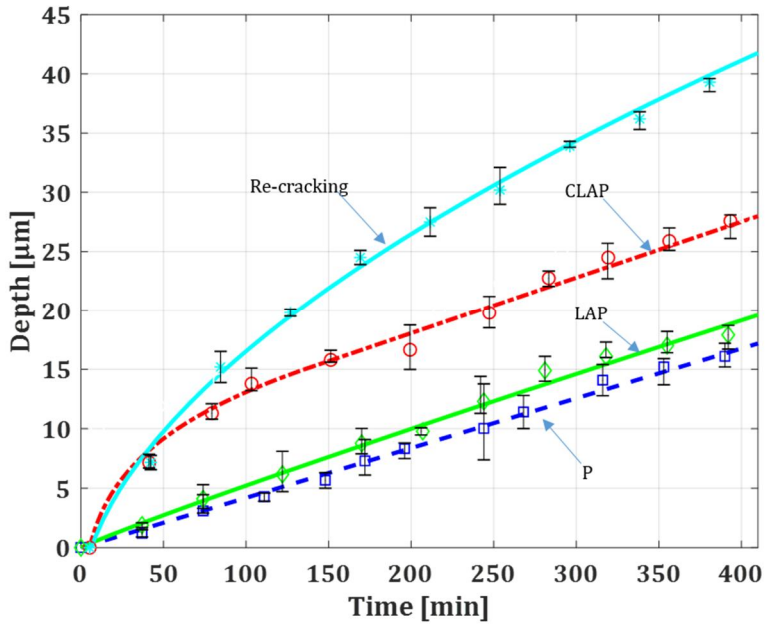

(a)

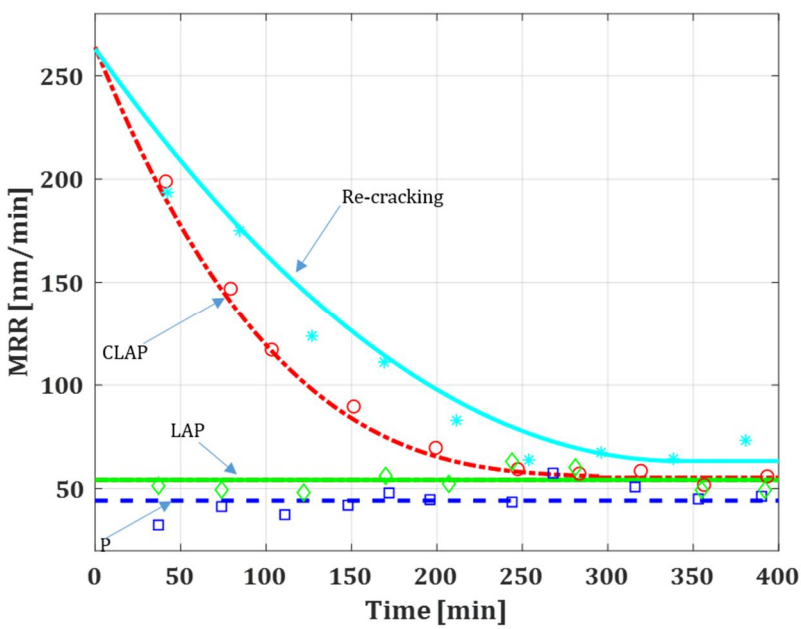

(b)

Figure 12. (a) Deepest polished point and (b) MRR of 4 different experiments

Chapter 4. Macro/Micro Channels

4.1. Macro/Micro Channels Design

Polishing process has several limitations, one of them is that all the area beneath the polishing pad will be machined and selective machining cannot be done without changing the design of the polishing tool. However, in this hybrid polishing process that was developed, the material removal rate between the laser pre-cracked regions and the non-pre-cracked regions is high enough to possibly selectively create 3D forms on silicon carbide surface.

In order to test this hybrid process's capability of creating macro/micro grooves on silicon carbide, 2 different experiments were conducted. An 'ㄹ' pattern with dimensions shown in figure 13 was laser cracked at 30% duty and subsequently laser assisted polished, and a similar pattern with variable width was similarly laser cracked and subsequently polished. A raster tool path of 0.05mm was used in both experiments.

The surface profile was measured using a surface profiler as in previous experiments. Moreover, in order to map the 3D surface, the surface profile was measured in 5 positions. The obtained data was then interpolated to obtain a 3D grid to illustrate the generated pattern.

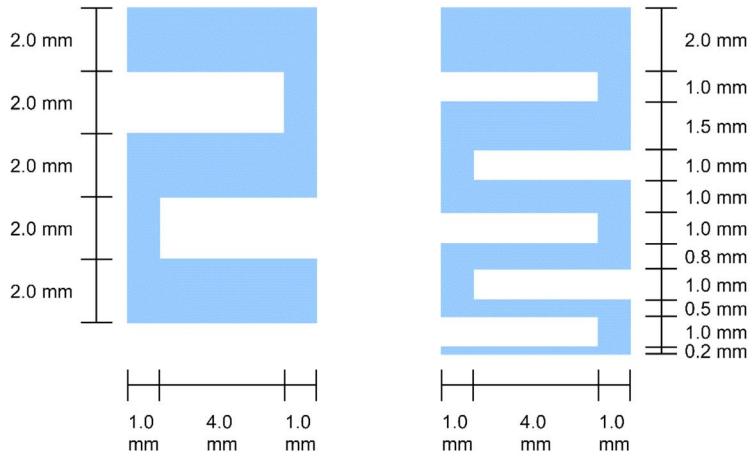

Figure 13. Diagram of the machined patterns

The results are shown in figure 14. As it can be seen, the pattern is not clearly seen, yet there is a higher material removal in some of the areas in which laser was previously irradiated. Due to the size of the polishing tool (radius=20mm), the material removal on the edges of the tool is significantly higher than in areas closer to the center. Therefore, before the tool reaches the lower part of the pattern tool path, the surface has already become reflective and the effect of laser assisted polishing is reduced on these areas.

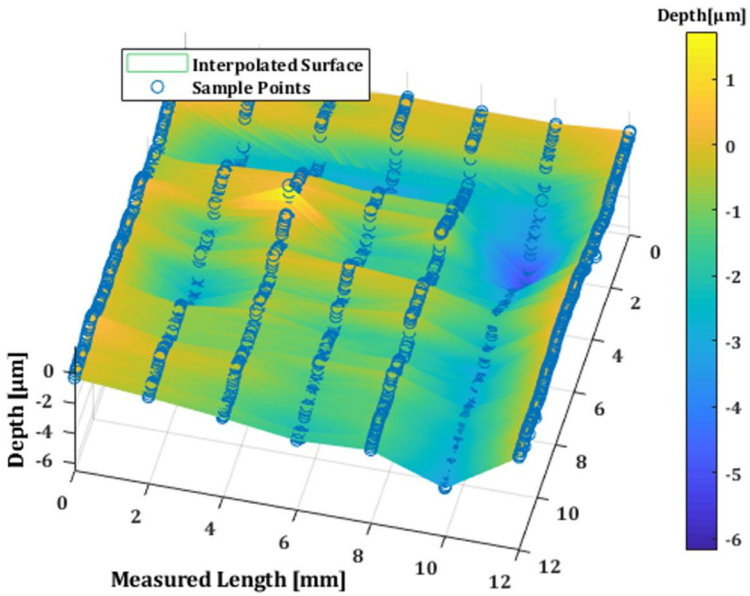

(a)

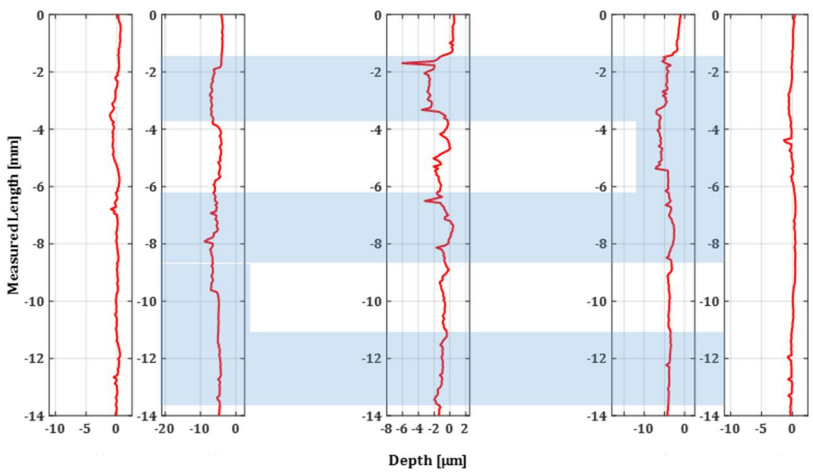

(b)

Figure 14. (a) 3D surface and (b) surface profile data of generated pattern

4.2. Tool Size Effect

Due to the size of the polishing pad, sharper patterns cannot be made. Taking into consideration these results, the polishing PDMS pad was modified. As shown in figure 15, the pad used for previous experiment was 20 mm in radius and the modified version was 12 mm. There is a limitation of the polishing pad diameter since a 10 mm diameter hole is required for the laser to be able to reach the sample's surface

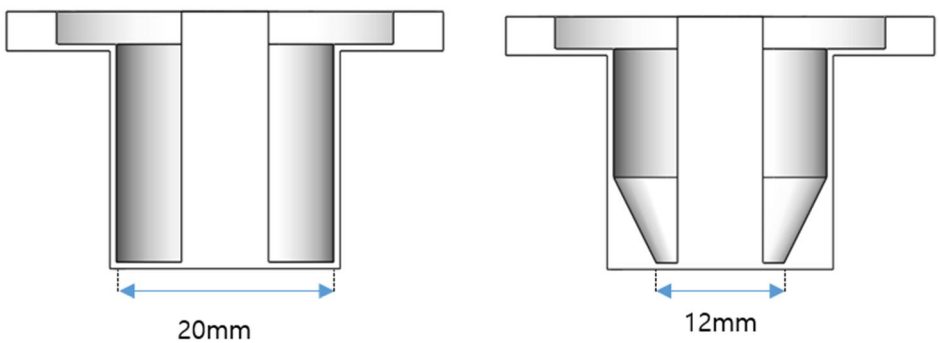

(a) (b)

Figure 15. (a) tool design for MRR experiment and failed pattern machining, and (b) modified tool for patterning.

The same experiment was conducted to investigate the effects of the modified tool size. Constant width and variable width channels were machined with this tool.

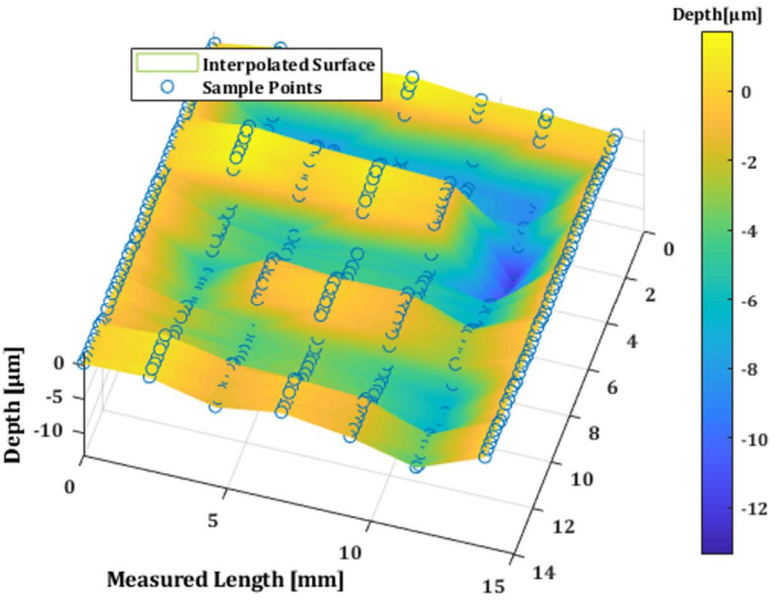

(a)

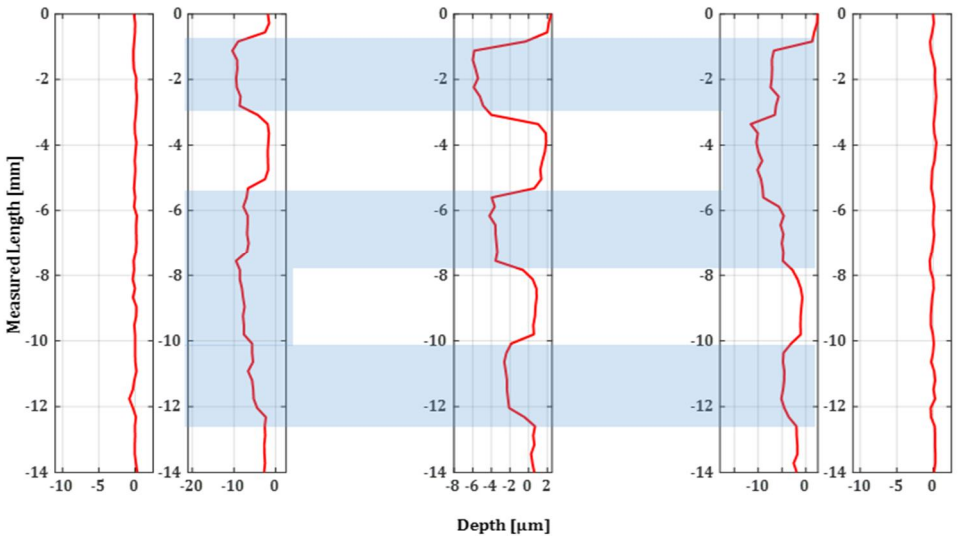

Figure 16. (a) 3D surface and (b) surface profile data of generated pattern with modified tool

(b)

4.3. Variable width channels

Previous experiments were conducted to validate the hypothesis that with a high material removal difference between pre-cracked and non-pre-cracked regions, specific patterns/shapes could be

generated. In order to study the size capabilities of this process, a variable width pattern was designed. As shown in figure 13, the width of the channels width was decreased from 2.0 mm to 0.2 mm.

The tool size and all other parameters including tool path and polishing time were the same as of the constant width pattern experiment.

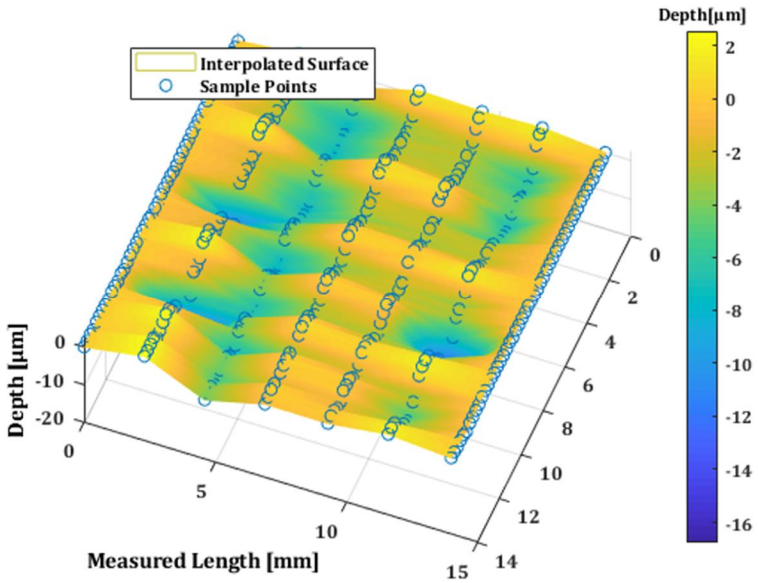

(a)

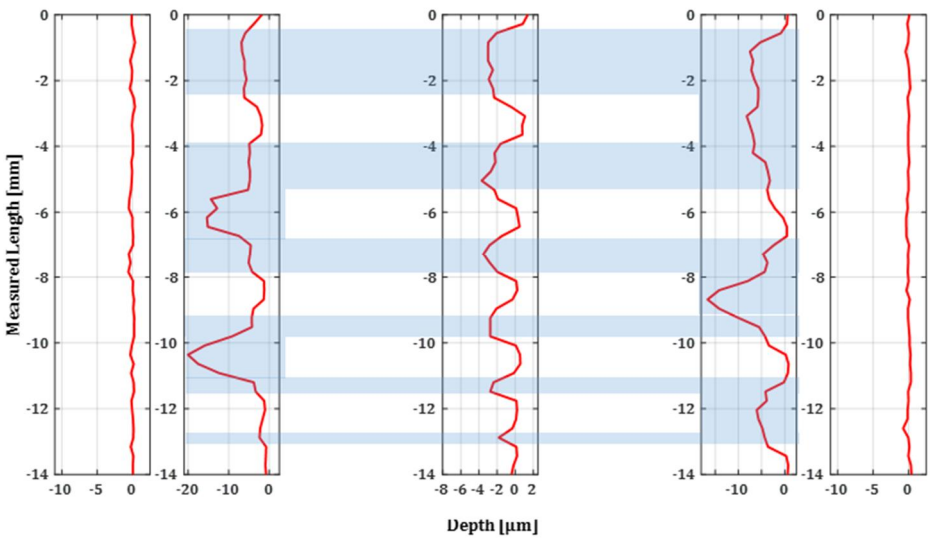

(b)

Figure 17. (a) 3D surface and (b) surface profile data of generated variable width pattern with modified tool

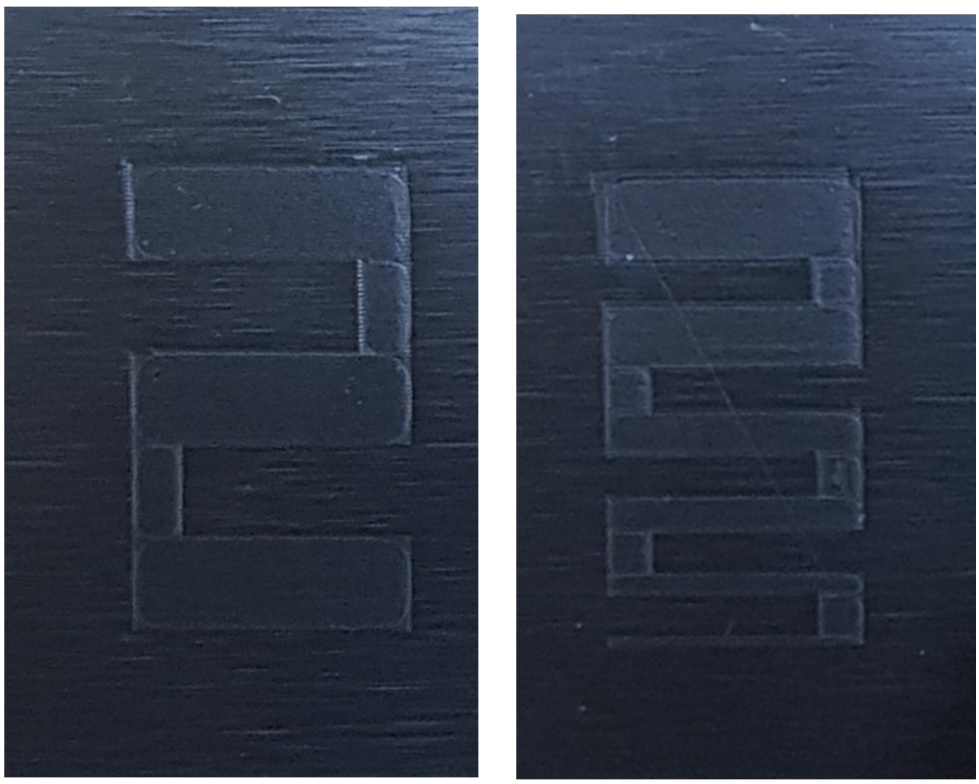

(a) (b)

Figure 18. Real image of (a) constant width channels and (b) variable width channels

4.4. Tool Path Effect

The results in figure 16 and figure 17 showed that it is possible to create grooves but laser cracking on small areas generates high heat accumulation and due to the small time it gives for heat to dissipate, it results on deep machined peaks. In order to evaluate this hypothesis, we increased the raster tool path width from 50 μm to 150 μm as shown in figure 19. This way, the laser effect on these areas could be reduce, and therefore obtain a more uniform depth along the pattern.

Surface profiler data shown in figure 20 shows that there was a significant effect of the laser raster tool path width on the

depth of cut. In order to create grooves with uniform depth, a parameter optimization has to be done to find the optimal raster tool path's width which leads to the deepest cracks with the less material vaporization.

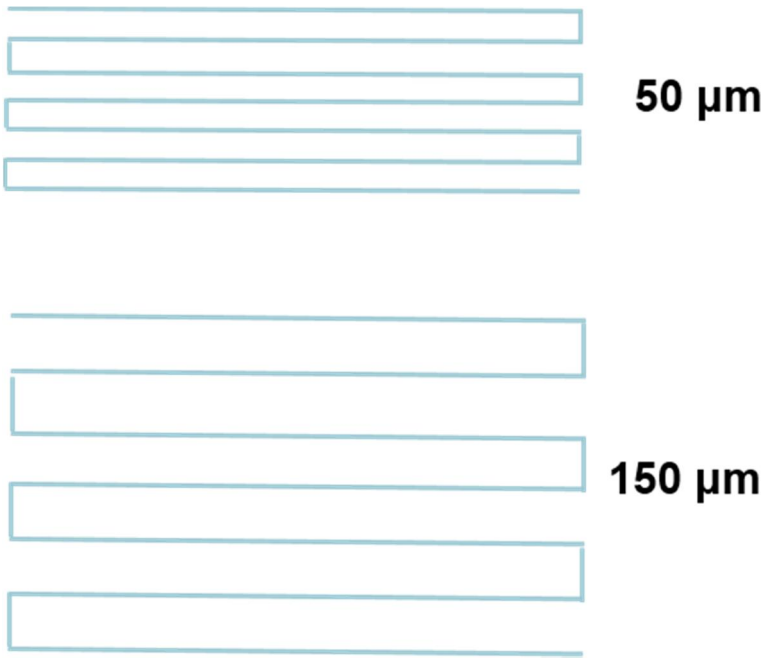

Figure 19. Modified raster tool path width

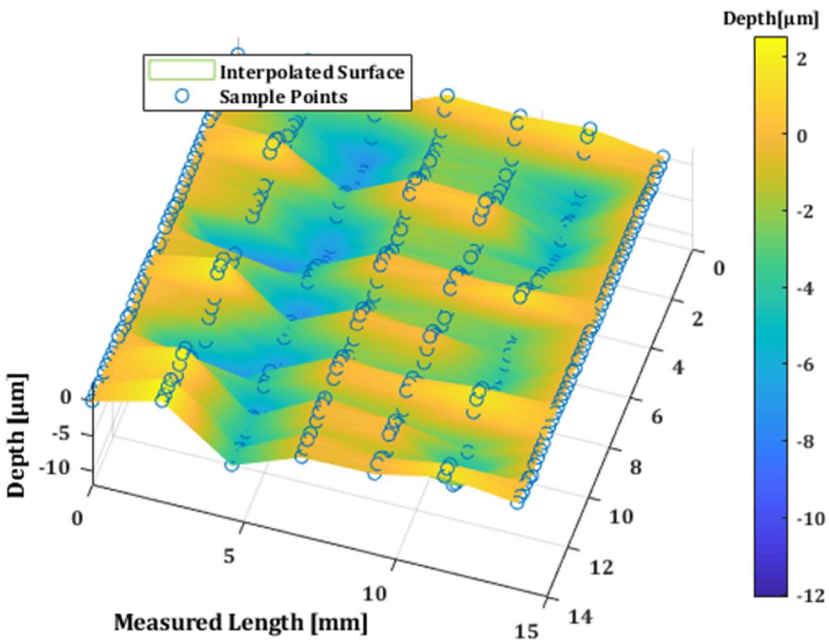

(a) 3D surface

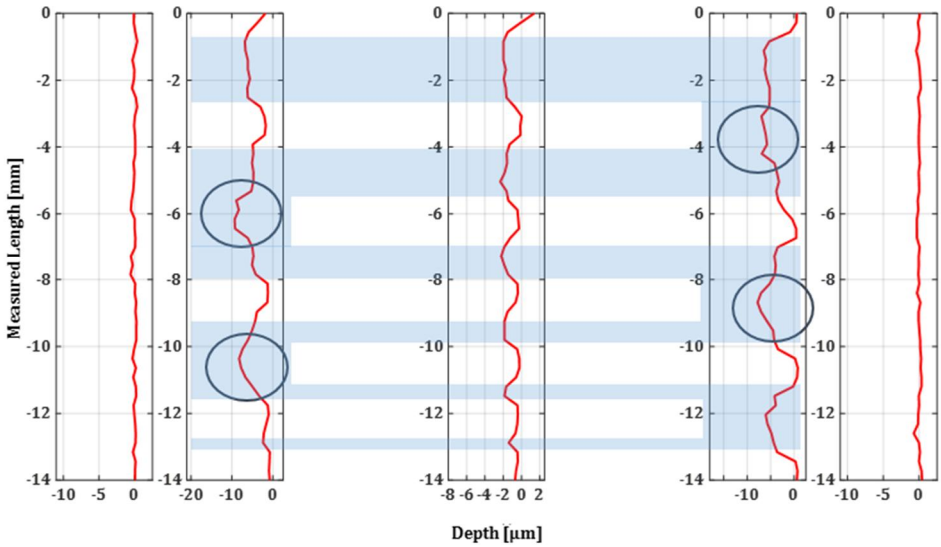

Figure 20. (a) 3D surface and (b) surface profile data of generated variable width pattern with modified tool and modified raster tool path

Chapter 5. Spherical Mirror Fabrication

5.1. Mirror design and Fabrication

It has been proved that this hybrid process can create different surface shapes depending on the tool path and how the sample is pre-cracked. In order to fabricate a concave spherical mirror, the pattern shown in figure 21 was pre-cracked. Concentric circles were pre-cracked using the same raster tool path as previous experiments (50 μm width). Each circle was cracked on top of the previous one in order to create an increasing crack depth gradient. This way, deeper cracks can be found in the center of the sample and less deep cracks in the outer part. By doing this, when polishing the sample, regardless the size and shape of the tool, the highest material removal will be located at the center of the sample and a concave spherical mirror can be fabricated.

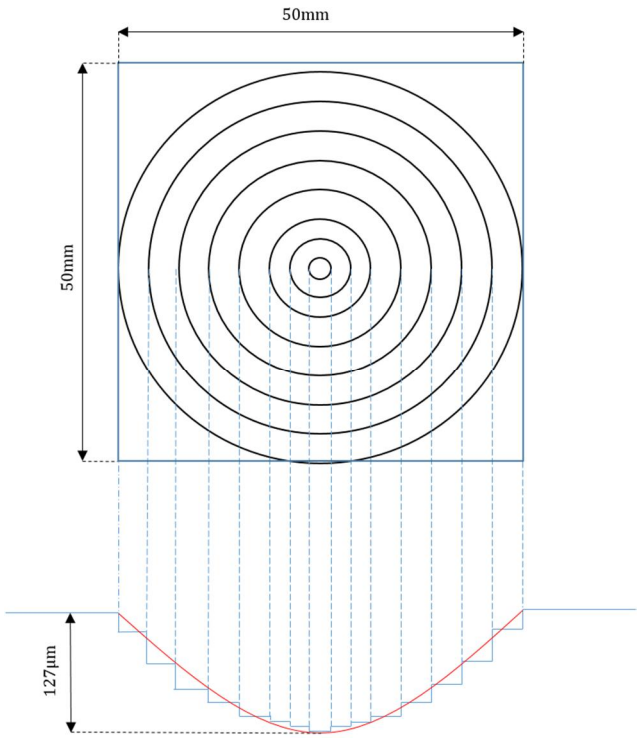

Figure 21. Spherical mirror fabrication diagram

The dimensions of the spherical mirror were 127 μm at its center, 50 mm of linear aperture and radius of curvature of 2200 mm. We chose these dimensions in order to match the commercial Newtonian telescope mirror shown in figure 22. The dimensions and parameters of this Newtonian telescope are shown in Table 3.

Figure 22. Commercial Newtonian telescope's mirror and holder

Table 3. Mirror parameters

Parameter [unit]	Value
Focal length	1100 mm
Linear aperture	150 mm
Primary mirror size	180 mm

On the contour of the concentric circles, we can see laser marks. These laser marks are deep pits that cannot be remove without further modification of the mirror shape. These mark are the result of the dwell time when the laser tool change direction after each raster path line. The dwell time is significantly high to create deep pits on the contour of the circles.

Figure 23. Fabricated concave spherical mirror by hybrid process

The profiler data was fitted with the commercial mirror

profile data. The fitting had a R−square=0.9321 and the final surface roughness was of 58 nm as shown in figure 24. Even though the R−square value is relatively good enough, in some areas a flat surface can be seen and this is due to the flat shaped tool.

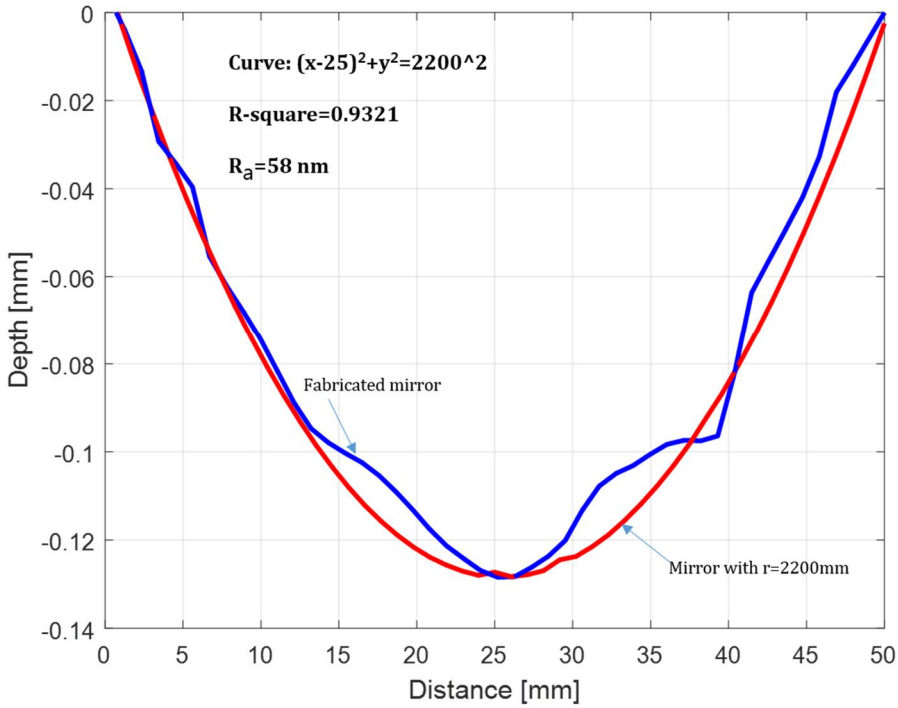

Figure 24. Surface profile of commercial mirror and fabricated mirror by hybrid process

5.2. Reflector of Newtonian Telescope

The Newtonian reflector is a classic mirror telescope design, and Isaac Newton first built this telescope in 1668. Newton was further developing an existing telescope design, one like the physicist Zucchi had already constructed in 1616, which employed a mirror. Newton's idea was to install a flat reflecting mirror into the telescope tube. Light would first enter the top of the telescope tube. At the lower end, there is a primary mirror that is either spherical or parabolic in configuration. This mirror reflects the light upwards. To prevent the image from being focused in front of the tube opening, there is a secondary mirror inside the top of the tube. This

is a plane mirror that deflects the light beam by 90°, thus directing it out the side of the tube. The light enters the focuser here, into an eyepiece that can be inserted for observation. Focusing takes place by turning a focus wheel on the focuser so that the eyepiece is moved towards or away from the telescope tube [22].

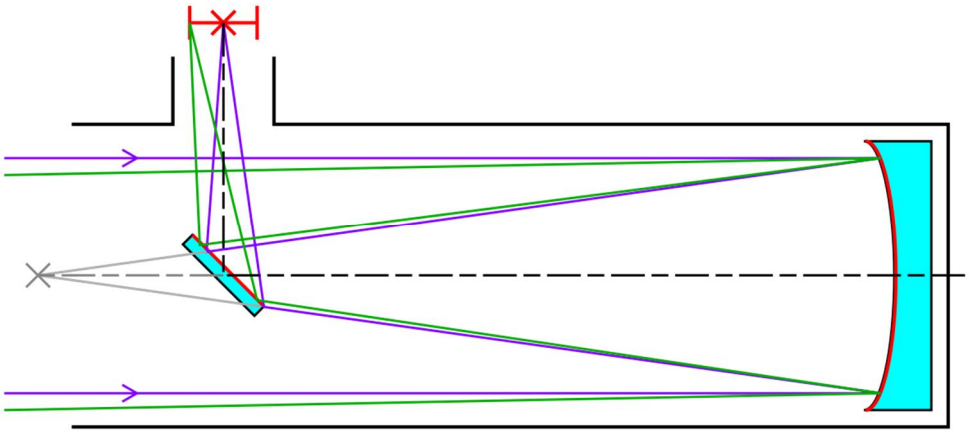

Figure 25. Newtonian telescope's principle

A commercial Newtonian telescope was used to test the fabricated concave spherical mirror. An ABS jig for the SiC mirror was manufactured by fused deposition modeling (FDM) (Dimension 768 SST, Stratasys). Figure 26 shows the SiC mirror together with the ABS jig

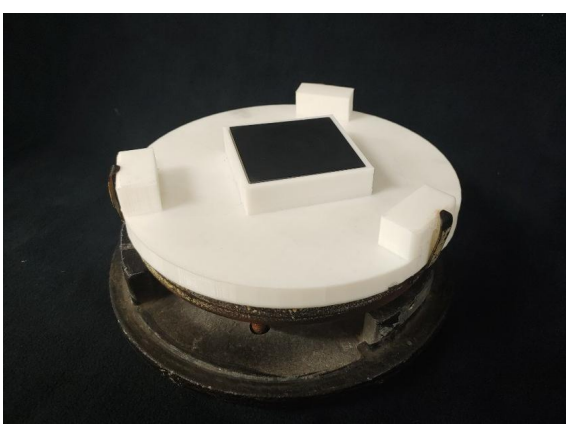

Figure 26. Fabricated SiC mirror and 3D printed jig

The fabricated SiC mirror was used to take the images shown in figure 27. Images were taken at different stages of fabrication to show the difference in magnification.

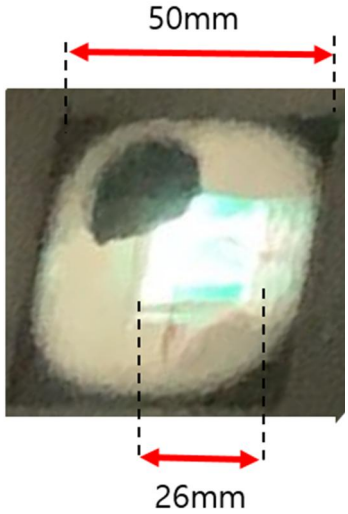

(a)

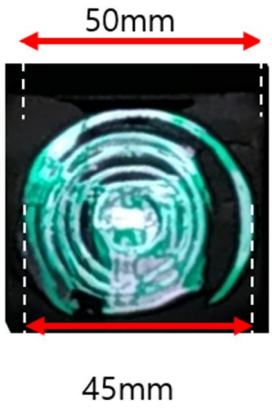

(b)

Figure 27. (a) image taken at early stage of polishing, and (b) image of mirror with curvature of 2200 mm radius

As it can be seen in figure 27, there are some circular marks in the pre-cracked shape. This laser marks are too deep to be removed by polishing process without modifying the shape of the mirror even further. Moreover, the shape of the mirror was not 100% equal to the commercial mirror. In order to fabricated a more accurate mirror, changes in experiment and tool design will have to be done.

Chapter 6. Conclusion

A hybrid polishing method was studied and different types of experiment were conducted in order to see the effects it has on the polishing process of Silicon Carbide (SiC). 3 different studies were done: material removal rate improvement, deep groves by hybrid polishing process and concave mirror fabrication.

The results showed that there is an improvement of the material removal rate by using this hybrid process over the conventional polishing process. The initial improvement is higher than 300% in comparison of conventional polishing, however, after the material removal rate reaches its constant value, the improvement is of 43% over conventional polishing.

Grooves were generated by cracking and subsequently laser assisted polishing on the cracked path. Deep groves of different sizes were generated. However, there are some limitations including the maximum width and the depth uniformity. These grooves could be generated over the whole surface of the sample and therefore improve its tribological properties.

Finally, a SiC mirror was fabricated in a shorter period of time than what conventional polishing process could have done. However, controlling the curvature of the mirror is not an easy task due to the flat shaped tool and lack of real time monitoring of the curvature.

Moreover, due to the flat shape, when the depth at the middle becomes significantly large, the tool mostly removes material at the sides and not at the middle, leading to a flat shape at this point.

More study has to be done related to the effect of surface reflectance and material removal rate. Also, modifying the raster tool path's width could significantly improve the non-uniform depth of the generated groove.

Bibliography

1. Johnson, J. S., Grobsky, K. D., & Bray, D. (2002, September). Rapid fabrication of lightweight silicon-carbide mirrors. In Optomechanical Design and Engineering 2002 (Vol. 4771, pp. 243-253).

2. Sun, S., Brandt, M. and Dargusch, M.S., 2010. Thermally enhanced machining of hard-to-machine materials—a review. International Journal of Machine Tools and Manufacture, 50(8), pp.663-680.

3. Suzuki, H., Kodera, S., Nakasuji, T., Ohta, T. and Syoji, K., 1998. Precision grinding of aspherical CVD-SiC molding die. International Journal of the Japan Society for Precision Engineering, 32(1), pp.25-30.

4. Evans, C.J., Paul, E., Dornfeld, D., Lucca, D.A., Byrne, G., Tricard, M., Klocke, F., Dambon, O. and Mullany, B.A., 2003. Material removal mechanisms in lapping and polishing. CIRP annals, 52(2), pp.611-633.

5. Kim, D.H. and Lee, C.M., 2016. A study on the laser-assisted ball-end milling of difficult-to-cut materials using a new back-and-forth preheating method. The International Journal of Advanced Manufacturing Technology, 85(5-8), pp.1825-1834.

6. Klocke, F. and Zunke, R., 2009. Removal mechanisms in polishing of silicon based advanced ceramics. CIRP annals, 58(1), pp.491-494.

7. Wegener, K., Bleicher, F., Krajnik, P., Hoffmeister, H.W. and Brecher, C., 2017. Recent developments in grinding machines. CIRP Annals, 66(2), pp.779-802.

8. Chen, B., Li, S., Deng, Z., Guo, B. and Zhao, Q., 2017. Grinding marks on ultra-precision grinding spherical and aspheric surfaces. International Journal of Precision Engineering and Manufacturing-Green Technology, 4(4), pp.419-429

9. Xing, Y., Deng, J., Zhang, K., Zhang, G. and Gao, H., 2014. Effect of femtosecond laser pretreatment on wear

resistance of Al2O3/TiC ceramic tools in dry cutting. International Journal of Refractory Metals and Hard Materials, 43, pp.291-301.

10. Zum Gahr, K.H., 1989. Sliding wear of ceramic-ceramic, ceramic-steel and steel-steel pairs in lubricated and unlubricated contact. Wear, 133(1), pp.1-22.

11. Tsumori, F., Hunt, S., Kudo, K., Osada, T. and Miura, H., 2016. Wavy Micro Channels in Micropatterned Ceramic Sheet Formed by Combined Process of Laser Beam Machining and Imprinting. Journal of the Japan Society of Powder and Powder Metallurgy, 63(7), pp.511-518.

12. Dandekar, C.R., Shin, Y.C. and Barnes, J., 2010. Machinability improvement of titanium alloy (Ti–6Al–4V) via LAM and hybrid machining. International Journal of Machine Tools and Manufacture, 50(2), pp.174-182.

13. Lauwers, B., Klocke, F., Klink, A., Tekkaya, A.E., Neugebauer, R. and Mcintosh, D., 2014. Hybrid processes in manufacturing. CIRP Annals, 63(2), pp.561-583.

14. Chu, W.S., Kim, M.S., Jang, K.H., Song, J.H., Rodrigue, H., Chun, D.M., Cho, Y.T., Ko, S.H., Cho, K.J., Cha, S.W. and Min, S., 2016. From design for manufacturing (DFM) to manufacturing for design (MFD) via hybrid manufacturing and smart factory: A review and perspective of paradigm shift. International Journal of Precision Engineering and Manufacturing-Green Technology, 3(2), pp.209-222.

15. Chu, W.S., Kim, C.S., Lee, H.T., Choi, J.O., Park, J.I., Song, J.H., Jang, K.H. and Ahn, S.H., 2014. Hybrid manufacturing in micro/nano scale: a review. International journal of precision engineering and manufacturing-green technology, 1(1), pp.75-92.

16. Jeon, Y., Park, H.W. and Lee, C.M., 2013. Current research trends in external energy assisted machining. International Journal of Precision Engineering and Manufacturing, 14(2), pp.337-342.

17. Kurniawan, R., Ali, S., Park, K.M., Li, C.P. and Ko, T.J., 2019. Development of a Three-Dimensional Ultrasonic

Elliptical Vibration Transducer (3D-UEVT) Based on Sandwiched Piezoelectric Actuator for Micro-grooving. International Journal of Precision Engineering and Manufacturing, pp.1-12.

18. Liang, Y., Chen, Y., Chen, B., Fan, B., Yan, C. and Fu, Y., 2019. Feasibility of Ultrasonic Vibration Assisted Grinding for Carbon Fiber Reinforced Polymer with Monolayer Brazed Grinding Tools. International Journal of Precision Engineering and Manufacturing, pp.1-12.

19. Cha, N.H. and Lee, C.M., 2015. A study on machining characteristics of silicon nitride with spline members in laser-assisted turn-mill. International Journal of Precision Engineering and Manufacturing, 16(13), pp.2691-2697.

20. Lee, C.M., Kim, D.H., Baek, J.T. and Kim, E.J., 2016. Laser assisted milling device: A review. International Journal of Precision Engineering and Manufacturing-Green Technology, 3(2), pp.199-208.

21. 김민철. (2019). 실리콘 카바이드 가공을 위한 레이저-폴리싱 융복합 공정.

22. VandeWettering, Mark T. (2001). "Telescope Basics".

국문 초록

실리콘 카바이드에 대한 CO_2 레이저 연마의 효과

파블로

서울대학교 공과대학원

기계항공공학부 기계공학전공

실리콘 카바이드 (SiC)는 일반적으로 사용되는 다른 유리 및 금속보다 많은 장점을 제공하기 때문에 오랫동안 고성능 광학 응용 분야에서 우수한 재료로 인정 받고 있다. SiC의 우수한 특성 중 일부는 매우 높은 고유 강성 (E / ρ), 높은 열 전도성 및 뛰어난 치수 안정성을 포함한다.

실리콘 카바이드에 대한 CO_2 레이저 연마와 레이저의 공구 경로의 효과가 조사하였다. 이 하이브리드 과정에는 먼저 원하는 패턴에 레이저 크랙을 냈다. 이어서, 레이저 보조 연마가 동일한 공구 경로에서 수행된다. 표면은 레이저 유도 크랙이 있는 영역과 크랙이 없는 영역에서 물질 제거에 있어 뚜렷한 차이를 보였다. 이러한 물질 제거의 높은 차이는 매크로 및 미세 패턴을 가공하기 위해서 사용되었다. 폭은 2 mm에서 200 μm까지, 그리고 깊이는 5 μm에서 20 μm까지 홈이 성공적으로 생성되었다. 또한, 이 하이브리드 과정은 Newtonian 망원경의 일부로 사용되는 구형 오목 거울을 가공하기 위해 사용되었다.

주요어: 연마, 하이브리드, 재료 제거율 (MRR), 패터닝

학번: 2017-26782